International Journal of Materials Science and Applications
2016; 5(3): 136-142
http://www.sciencepublishinggroup.com/j/ijmsa
doi: 10.11648/j.ijmsa.20160503.14
ISSN: 2327-2635 (Print); ISSN: 2327-2643 (Online)

Synthesis of $Li[Li_{0.13}Mn_{0.464}Ni_{0.203}Co_{0.203}]O_2$ Cathode Material by Hydrothermal Treatment Method

Wang Meng[1, 2, *], Li Wei[1], Yang Tao[1], Wu Feng[2]

[1]Jiangsu Chunlan Clean Energy Academy CO., LTD., Jiangsu, China

[2]School of Materials Science and Engineering, Beijing Institute of Technology, Beijing, China

Email address:

manyou2005@163.com (Wang Meng)

[*]Corresponding author

To cite this article:

Wang Meng, Li Wei, Yang Tao, Wu Feng. Synthesis of $Li[Li_{0.13}Mn_{0.464}Ni_{0.203}Co_{0.203}]O_2$ Cathode Material by Hydrothermal Treatment Method. *International Journal of Materials Science and Applications*. Vol. 5, No. 3, 2016, pp. 136-142. doi: 10.11648/j.ijmsa.20160503.14

Received: April 26, 2016; **Accepted**: May 28, 2016; **Published**: June 7, 2016

Abstract: The layered Li-rich $Li[Li_{0.13}Mn_{0.464}Ni_{0.203}Co_{0.203}]O_2$ cathode material was successfully synthesized via a hydrothermal treatment on the precursor method. X-ray diffraction spectrometry (XRD) and scanning electron microscopy (SEM) were used to characterize the structure and micromorphology of the materials. Meanwhile, charge-discharge test and electrochemical impedance spectroscopy (EIS) were employed to explore its electrochemical performance. The results indicate that the $Li[Li_{0.13}Mn_{0.464}Ni_{0.203}Co_{0.203}]O_2$ material possesses a layered α-$NaFeO_2$ structure and exhibits excellent electrochemical performance. The initial discharge capacity is 235.9 $mAh \cdot g^{-1}$ in the voltage range of 2.0-4.8 V at 0.1 C. And it exhibits the capacity retention of 94.1% after 50 cycles. The hydrothermal treatment not only shortens the calcination time, but also can greatly improve the electrochemical performance of the material.

Keywords: Lithium-ion Battery, Hydrothermal, Li-rich, Cathode Material

1. Introduction

Lithium ion batteries have been regarded as one of promising power source candidates for electric vehicles in recent years [1-3]. However, the discharge capacities of traditional cathode materials, such as layered $LiCoO_2$, $LiMn_{1/3}Ni_{1/3}Co_{1/3}O_2$, olivine $LiFePO_4$, and spinel $LiMn_2O_4$, cannot entirely meet the capacity requirements of the electric vehicle. Therefore, the development of alternative low cost cathode materials with high specific capacity becomes the inevitable trend. Recently, Li-rich solid solution $xLi_2MnO_3 \cdot (1-x)LiMO_2$ (M = Co, Mn, Ni, etc.) cathode materials have received great attention for their large capacity over 200 $mAh \cdot g^{-1}$ when charged to high potentials (typically >4.5 V) [4-10]. Although Li-rich cathode materials show extraordinarily high discharge capacity, they are still far from real applications because of several unsolved issues. Such as the low rate capability, the thick solid electrolyte inter-facial (SEI) layer formed when operating at high voltages and structural evolution while cycling [11].

The electrochemical performance of $xLi_2MnO_3 \cdot (1-x)LiMO_2$ is greatly depends on the synthesis method. Because the important roles in the electrochemical performance of the material, such as crystallinity, phase purity, particle morphology, grain size, surface area, and cation distribution in the structure are all rely on synthesis method [12-14]. A lot of different preparation methods have been recently developed to prepare high performance $xLi_2MnO_3 \cdot (1-x)LiMO_2$ materials, such as co-precipitation method [15-18], sol-gel method [19, 20], combustion method [21-23], template method [24] and so on. Among these methods, hydroxide and carbonate co-precipitation methods are widely used because they can mix the raw materials at molecular level. However, a major drawback of the hydroxide co-precipitation method is that Mn^{2+} can be easily oxidized to Mn^{3+}, then result in impure phases in final product [25]. However, carbonate co-precipitation can keep Mn in divalent oxidation state since the pH value of solution is kept around 8, which is less harsh than that in hydroxide process (pH=11) [7]. It is reported the precursors play important roles on electrochemical performances of the cathode materials [26-28]. In this work, we developed a simple method of hydrothermal treatment on the carbonate precursor to

synthesize nanostructured $Li[Li_{0.13}Mn_{0.464}Ni_{0.203}Co_{0.203}]O_2$ particles. The structure, morphology and electrochemical properties of the material were investigated.

2. Experiment

To synthesize lithium-rich $Li[Li_{0.13}Mn_{0.464}Ni_{0.203}Co_{0.203}]O_2$ cathode material, $MnSO_4·H_2O$, $NiSO_4·6H_2O$ and $CoSO_4·7H_2O$ were used as starting materials. The synthesis process is shown in Figure 1. An aqueous mixed solution of and $MnSO_4·H_2O$, $NiSO_4·6H_2O$ and $CoSO_4·7H_2O$ (cationic ratio of Mn: Ni: Co = 0.464: 0.203: 0.203) with total metal ion concentration of 1.0 mol·L^{-1} was pumped into a continuously stirred tank reactor. At the same time, 1.0 mol·L^{-1} Na_2CO_3 aqueous solution as a precipitant and NH_4OH aqueous solution as a chelating agent were also separately fed into the reactor. The pH of the solution is 8.0, the operation temperature is 55°C and the stirring speed of the mixture in the reactor were carefully controlled at 500 r·min^{-1}. After the precipitation was completely finished, the obtained $[Mn_{0.464}Ni_{0.203}Co_{0.203}](CO_3)_{0.87}$ particles were filtered and washed by deionized water. $LiNO_3$ (5% excess) was dissolved in deionized water and $[Mn_{0.464}Ni_{0.203}Co_{0.203}](CO_3)_{0.87}$ was added to form 185 ml mixed suspension. Then it was transferred into a 200 ml Teflon beaker autoclave. The autoclave was sealed and heated at 180°C under auto-generated pressure for 30 h, and then transferred to a glass beaker and heated at 85°C with continuous stirring until the water was almost evaporated. The obtained mixture dried at 100°C overnight, then calcined at 850°C for 8 h in air to obtain the final products, named the sample A. For comparison, the sample B was prepared by the carbonate co-precipitation method without hydrothermal treatment on the carbonate precursor.

The structure characterization with X-ray diffraction (XRD) was carried out using Rigaku Ultima IV-185 with Cu K_α radiation between 10 and 80° 2θ at a scan rate of 8° min^{-1}. The morphology of the materials was observed by a FEI Quanta 250 scanning electron microscope (SEM).

The electrochemical properties of $Li[Li_{0.13}Mn_{0.464}Ni_{0.203}Co_{0.203}]O_2$ were examined in the CR2025 coin type cells. Electrodes were prepared by mixing of 80 wt.% active material, 10 wt.% carbon black and 10 wt.% polyvinylidene fluoride in N-methyl-2-pyrrolidone. The obtained slurry was coated on aluminum foil and dried in a vacuum oven at 55°C for 8 h. CR2025-type coin cells were fabricated by using Li metal as the counter electrode in an argon-filled glove box. The electrolyte solution was a 1 M $LiPF_6$ in ethylene carbonate (EC) - dimethyl carbonate (DMC) (1:1, v/v). The galvanostatic charge-discharge tests were controlled between 2.0 and 4.8 V using CT2001A Land instrument at room temperature. The electrochemical impedance spectroscopy (EIS) measurement was conducted by a CHI impedance analyzer, using an amplitude voltage 5 mV and the frequency range was 10^{-2}- 10^5 Hz.

Figure 1. *The illustration of the synthesis process.*

3. Results and Discussion

3.1. Crystal Structure and Morphology

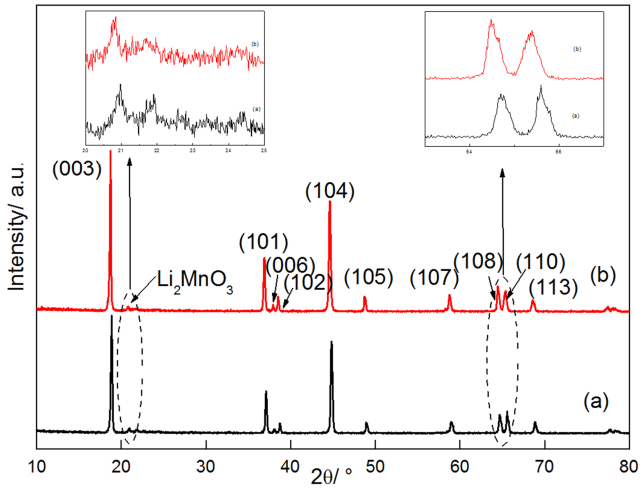

Figure 2. *XRD pattern of (a) sample A and (b) sample B.*

Figure 2 shows the X-ray diffraction pattern of $Li[Li_{0.13}Mn_{0.464}Ni_{0.203}Co_{0.203}]O_2$. Both of the composites show a typical α-$NaFeO_2$ layered hexagonal structure with *R-3m* space group. The (006)/(102) and (108)/(110) doublets are clear split, which indicate the as-prepared cathode materials have a well-organized layered structure [29]. The magnified XRD patterns between 20° and 25° are inserted in Figure 2 (left). Several weak peaks around 20°-25° are related to the existence of Li_2MnO_3 [30-32]. The intensity ration of $I_{(003)}/I_{(104)}$ represents the cation mixing degree of the layered structure [33-35]. When the value of $I_{(003)}/I_{(104)}$> 1.2, the cation mixing phenomenon is very weak [36]. In this work, the $I_{(003)}/I_{(104)}$ values of the sample A and B are 1.29 and 1.22, respectively. The sample A has a high $I_{(003)}/I_{(104)}$ value which indicates this material has a higher structural order than the sample B.

Another important parameter related to the material structure order is the *R*-factor ($R=[I_{(102)}/I_{(006)}]/I_{(101)}$). A lower *R* value represents better hexagonal order [37]. The *R* value of the sample A (0.30) is lower than that of the sample B (0.36), which indicates the sample A has a better hexagonal order than the sample B. Consequently, the sample A prepared by hydrothermal treatment has good crystallinity. This is due to a short calcining time (8 h) is sufficient for the crystal growth of the sample A, but is not enough long for the sample B.

The SEM images of the $Li[Li_{0.13}Mn_{0.464}Ni_{0.203}Co_{0.203}]O_2$ prepared by different methods are shown in Figure 3. As can be seen from the SEM images, the sample A is comprised of well crystallized particles with a slight aggregation. Comparatively, the particles edge of the sample B is not obviously sharp for the short calcination time. In addition, the agglomerates of primary particles in the sample B is much more close than that in the sample A. In general, a lower degree of agglomeration can lead to a better electrochemical performance [38]. The particle size distribution of the sample B is between 200 and 500 nm, while that of sample A is 400 and 800 nm. It can be seen that the hydrothermal treatment makes the particles evenly growing which will be good for high tap density. Moreover, such nanosized particles have a high surface area and provide a short diffusion path for Li^+ insertion/extraction and also for the diffusive transport of the oxygen ion vacancies. Thus, the electrochemical performance, especially the high rate capacity can be improved [39].

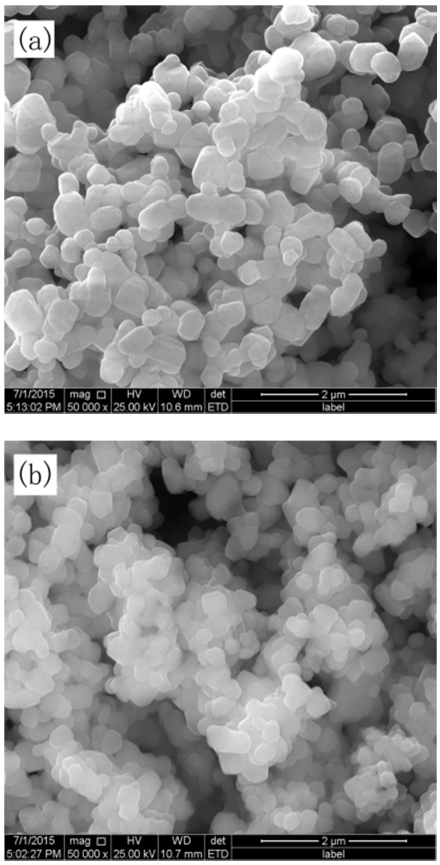

Figure 3. *SEM images of the (a) sample A and (b) sample B.*

3.2. Electrochemical Properties

Figure 4 shows the initial and second charge–discharge curves of $Li[Li_{0.13}Mn_{0.464}Ni_{0.203}Co_{0.203}]O_2$ at a current density of 0.1 C (1.0 C = 250 $mA \cdot g^{-1}$) in the voltage range of 2.0-4.8 V at room temperature. As can be seen from the Fig. 4, there are two plateaus in the initial charge curve: one is at about 4.0 V and the other one is at about 4.5 V. The former plateau is the Li-extraction from the structure of space group *R-3m* accompanying with the reactions of $Ni^{2+}/^{4+}$and $Co^{3+}/^{4+}$ [40]. The latter plateau is about the electrochemical removal of Li_2O from the structure which is related to the activation of Li_2MnO_3. This is responsible for the large irreversible capacity in the first cycle [41]. As shown in Figure 4, the charge platform at 4.5 V disappears in the second cycle. It attributes to the irreversible activation of Li_2MnO_3, which is agreement with other literature reports [42-45]. The initial discharge capacity and coulombic efficiency of the sample A are 235.9 $mAh \cdot g^{-1}$ and 73.1%, respectively. While those of the sample B are only 205.7 $mAh \cdot g^{-1}$ and 66.8%, respectively. The better electrochemical performance of the sample A can be due to the ordered layered structure. One of the great merits of the hydrothermal treatment on the carbonate precursor is it can prepared material with good electrochemical properties in a short period of calcination time [46]. The Li-rich layered oxides obtained via traditional carbonate coprecipitation method by other reports have to be heated at 900°C for more than 12 h [41, 47, 48]. In our study, materials with excellent electrochemical properties can be obtained by calcining only 8 hours.

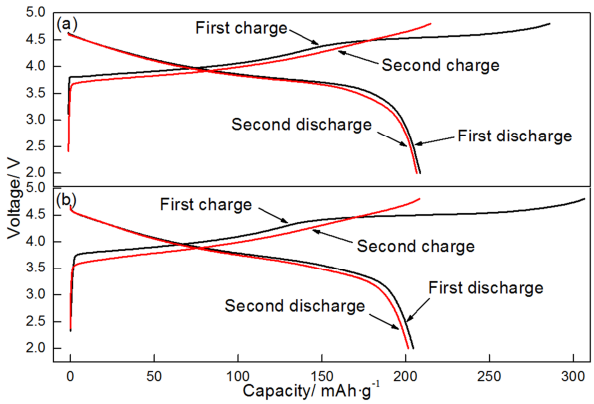

Figure 4. *The first and second charge-discharge curves of the (a) sample A and (b) sample B.*

Figure 5 shows the cycling performance and corresponding coulombic efficiency of the materials in the voltage range of 2.0-4.8 V at a current density of 0.1 C. It is demonstrates the sample A has a higher discharge capacity than the sample B. And after 50 cycles, the discharge capacity of the sample A also remains 221.9 $mAh \cdot g^{-1}$ with the capacity retention of 94.1%. While the capacity retention of the sample B is only 89.8% after 50 cycles. As given in Figure 5, both samples show coulombic efficiencies greater than 98% after the first cycle. The high discharge capacity and stable cycling performance of the sample A can be attributed to its

well-defined structure. As discussed above, the hydrothermal treatment on the carbonate precursor is beneficial to prepare the highly ordered layered structure and low degree of cation mixing, and they are benefit to the electrochemical performance. The decrease in discharge capacity is apparent for both samples, which is attributed to two main reasons. One is the dissolution of the metal ions, especially the Mn^{3+} during the charge-discharge process. It will redeposit on the surface of the oxide particle and seriously destroy the oxide surface to form an unsatisfactory surface film. This may be the main reason for the low capacity retention of the Li-rich layered oxides. The other is the Jahn-Teller distortion during the cycling process [49-52].

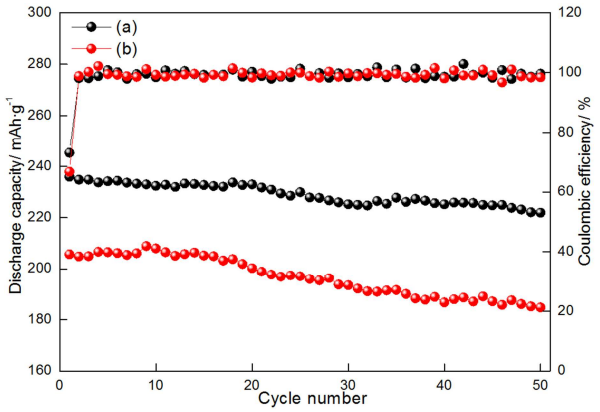

Figure 5. *Cycling performance of the (a) sample A and (b) sample B.*

The Midpoint voltages (MPVs) of discharge at different cycles of the sample A and B are shown in Figure 6. It can be observed from Figure 6, the discharge MPVs of the sample A is higher than that of the sample B. With the increases of cycle number, the MPVs of discharge decrease fast for the sample B. At 50th cycle, the MPV of discharge for the sample B is only 3.41 V, which is much lower than that of the sample A (3.65 V). The significantly reduced midpoint voltage and increased polarization of the materials after cycling would be partly due to the deterioration of electrode/electrolyte interface caused by side reaction with the electrolyte. This can be proved from the later EIS test.

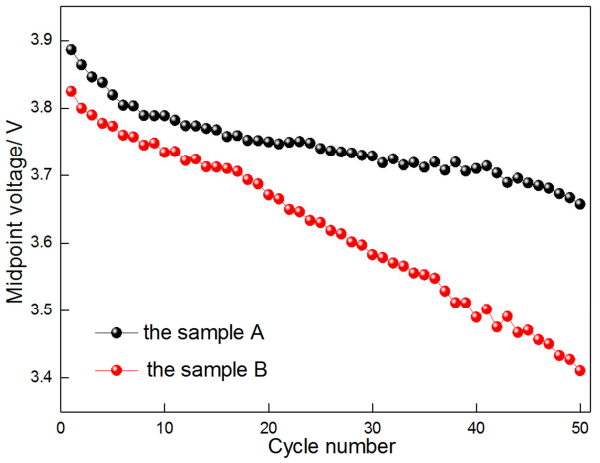

Figure 6. *Midpoint voltages of charge/discharge at different cycles at 0.1 C.*

The rate capability is an important factor for battery performance because the charge time of batteries in portable electric devices depends on the rate of Li^+ extraction out and insertion into the cathode [22]. Figure 7 presents the rate capability of the sample A and B between 2.0 and 4.8 V at room temperature. And retention of the discharge capacity are also presented in Figure 7. Each cell was charged at 0.1 C and then discharged at different rates from 0.1 to 2.0 C. Obviously, the sample A exhibits a higher discharge capacity and better rate capability at any C rates than the sample B. When the current density increased from 0.1 to 2.0 C, the discharge capacity of the sample A drops from 235.9 to 195.1 $mAh \cdot g^{-1}$ and the capacity retention is 82.7%. While the sample B shows a low discharge capacity of 155.9 $mAh \cdot g^{-1}$ at 2.0 C, which is only 75.8% of the discharge capacity at 0.1 C. The enhanced rate capacity of the sample A is mainly attributed to the less aggregation particles which could provide more paths for lithium-ion de/intercalation.

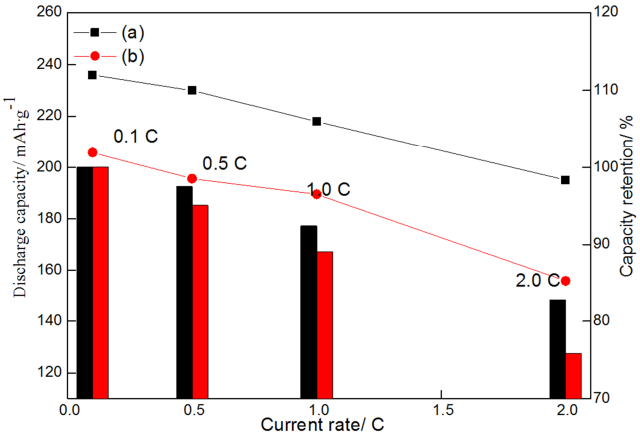

Figure 7. *The discharge capacities and capacity retention of the (a) sample A and (b) sample B at different current rate.*

Electrochemical impedance spectroscopy (EIS) of the fully charged coin cells (4.8 V) is measured to investigate the interface reaction and the process of lithium intercalation/deintercalation into electrode [53, 54]. The EIS profiles of the sample A were obtained when the cell cycled for 1 and 50 times respectively at 0.1 C between 2.0-4.8 V. The EIS profiles of the sample A are presented in Figure 8. The impedance spectra curves are composed of two parts, a depressed semicircle in high frequency region and a sloping line in low frequency region. Generally, the high frequency semicircle is related to the impedance due to Li^+ ion migration through the interfacial layer between solid and electrolyte. The low frequency line is ascribed to the solid-state diffusion of Li^+ ion in the positive electrode [55, 56]. An equivalent electrical circuit was inset in Figure 8. The fitting parameters involve the resistance of the electrode systerm (R_s), charge transfer resistance (R_{ct}) due to lithium intercalation/de-intercalation process, the non-ideal double layer capacitance (CPE) and the Warburg element (Z_w) corresponding to the straight sloping line at the low frequency region [47, 57]. It can be seen that, the charge transfer resistance increases as the cycle proceeds. The Nyquist plots is 149.6 Ω at first cycle then increases to 217.1 Ω

after 50 cycles. One reason is that when the charge potential gets as high as 4.8 V, some side reactions will occur between the active material and electrolyte and this will destroy the structure of the material to some extent. Therefore, the bulk structural changes result in the increase of impedance value [45, 58].

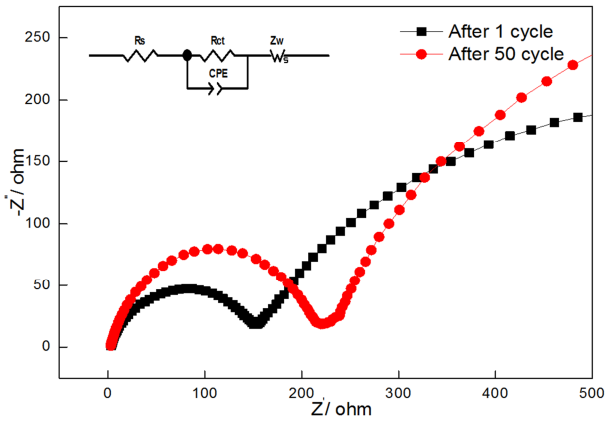

Figure 8. *Electrochemical impedence spectroscopy (EIS) Nyquist plots of the sample A at 4.8 V.*

4. Conclusion

In conclusion, the $Li[Li_{0.13}Mn_{0.464}Ni_{0.203}Co_{0.203}]O_2$ cathode material has been successfully prepared via a hydrothermal reaction route and a short calcination process. This method could shorten calcination time and reduce the energy consumption compared with traditional process. The material is proven to have a well-organized layered structured and the particle size distribution is 400-800 nm. The initial discharge capacity is 235.9 $mAh \cdot g^{-1}$ at 0.1 C. Rate test shows that the capacity retention at 2.0 C is 82.7% of the discharge capacity at 0.1 C. The good electrochemical performance of the materials prepared by this method can be attributed to the highly ordered layered structure and low amount of cation mixing.

References

[1] J. Y. Kim, and D. Y. Lim, "Surface-Modified Membrane as A Separator for Lithium-Ion Polymer Battery," Energies, vol. 3, pp. 866-885

[2] F. Y. Cheng, Z. L. Tao, J. Liang, and J. Chen, "Template-Directed Materials for Rechargeable Lithium-ion Batteries," Chem. Mater., Vol. 20, pp. 667-681

[3] M. S. Whittingham, "Lithium Batteries and Cathode Materials," Chem. Rev., Vol. 104, pp. 4271-4302

[4] C. Delmas, G. Prado, A. Rougier, E. Suard, and L. Fournes, "Effect of iron on the electrochemical behaviour of lithium nickelate: from $LiNiO_2$ to 2D-$LiFeO_2$," Solid State Ionics, Vol. 135, pp. 71-79

[5] C. Jaephil, and P. Byungwoo, "Preparation and electrochemical/thermal properties of $LiNi_{0.74}Co_{0.26}O_2$ cathode material," J. Power Sources, Vol. 92, pp. 35-39

[6] T. Ohzuku, and N. Yabuuchi, "Novel lithium insertion material of $LiCo_{1/3}Ni_{1/3}Mn_{1/3}O_2$ for advanced lithium-ion batteries," J. Power Sources, Vol. 119, pp. 171-174

[7] C. S. Johnson, N. Li, and C. Lefief, "Anomalous capacity and cycling stability of $xLi_2MnO_3 \cdot (1-x)LiMO_2$ electrodes (M = Mn, Ni, Co) in lithium batteries at 50°C," Electrochem. Commun., Vol. 9, pp. 787-795

[8] Y. Wu, and A. Manthiram, "High Capacity, Surface-Modified Layered $Li[Li_{(1-x)/3}Mn_{(2-x)/3}Ni_{x/3}Co_{x/3}]O_2$ Cathodes with Low Irreversible Capacity Loss," Electrochem. Solid-State Lett., Vol. 9, pp. A221-A224

[9] Y. Zhang, P. Hou, E. Zhou, X. Shi, X. Wang, D. Song, J. Guo, and L. Zhang, " Pre-heat treatment of carbonate precursor firstly in nitrogen and then oxygen atmospheres: A new procedure to improve tap density of high-performance cathode material $Li_{1.167}(Ni_{0.139}Co_{0.139}Mn_{0.556})O_2$ for lithium ion batteries," J. Power Sources, Vol. 292, pp. 58-65

[10] E. Zhao, X. Liu, Z. Hu, L. Sun, and X. Xiao, "Facile synthesis and enhanced electrochemical performances of Li_2TiO_3-coated lithium-rich layered $Li_{1.13}Ni_{0.30}Mn_{0.57}O_2$ cathode materials for lithium-ion batteries," J. Power Sources, Vol. 294, pp. 141-149

[11] X. Wei, S. Zhang, Z. Du, P. Yang, J. Wang, and Y. Ren, "Electrochemical performance of high-capacity nanostructured $Li[Li_{0.2}Mn_{0.54}Ni_{0.13}Co_{0.13}]O_2$ cathode material for lithium ion battery by hydrothermal method," Electrochim. Acta, Vol. 107, pp. 549-554

[12] C. H. Song, A. M. Stephan, A. Kim, and K. S. Nahm, "Influence of Solvents on the Structural and Electrochemical Properties of $Li[Li_{0.2}Ni_{0.1}Co_{0.2}Mn_{0.5}]O_2$ Prepared by a Solvothermal Reaction Method," J. Electrochem. Soc., Vol. 153, pp. A390-A395

[13] H. Huang, and P. G. Bruce, A 4 V Lithium Manganese Oxide Cathode for Rocking-Chair Lithium-Ion Cells, J. Electrochem. Soc., Vol. 141, pp. L106-L107

[14] D. Chen, Q. Yu, X. Xiang, M. Chen, Z. Chen, S. Song, L. Xiong, Y. Liao, L. Xing, and W. Li, "Porous layered lithium-rich oxide nanorods: Synthesis and performances as cathode of lithium ion battery," Electrochim. Acta, Vol. 154, pp. 83-93

[15] J. Gao, J. Kim, and A. Manthiram, "High capacity $Li[Li_{0.2}Mn_{0.54}Ni_{0.13}Co_{0.13}]O_2$-$V_2O_5$ composite cathodes with low irreversible capacity loss for lithium ion batteries," Electrochem. Commun., Vol. 11, pp. 84-86

[16] J. H. Lim, H. Bang, K. S. Lee, K. Amine, and Y. K. Sun, "Electrochemical characterization of Li_2MnO_3-$Li[Ni_{1/3}Co_{1/3}Mn_{1/3}]O_2$-$LiNiO_2$ cathode synthesized via co-precipitation for lithium secondary batteries," J. Power Sources, Vol. 189, pp. 571-575

[17] S. H. Kang, and M. M. Thackeray, "Enhancing the rate capability of high capacity $xLi_2MnO_3 \cdot (1-x)LiMO_2$ (M=Mn, Ni, Co) electrodes by Li-Ni-PO_4 treatment," Electrochem. Commun., Vol. 11, pp. 748-751

[18] X. J. Guo, Y. X. Li, M. Zheng, J. M. Zheng, J. Li, Z. L. Gong, and Y. Yang, "Structural and electrochemical characterization of $xLi[Li_{1/3}Mn_{2/3}]O_2 \cdot (1-x)Li[Ni_{1/3}Mn_{1/3}Co_{1/3}]O_2$ ($0 \le x \le 0.9$) as cathode materials for lithium ion batteries," J. Power Sources, Vol. 184, pp. 414-419

[19] J. M. Zheng, X. B. Wu, and Y. Yang, "A comparison of preparation method on the electrochemical performance of cathode material $Li[Li_{0.2}Mn_{0.54}Ni_{0.13}Co_{0.13}]O_2$ for lithium ion battery," Electrochim. Acta, Vol. 56, pp. 3071-3078

[20] S. H. Kang, P. Kempgens, S. Greenbaum, A. J. Kropf, K. Amine, and M. M. Thackeray, "Interpreting the structural and electrochemical complexity of $0.5Li_2MnO_3 \cdot 0.5LiMO_2$ electrodes for lithium batteries ($M=Mn_{0.5-x}Ni_{0.5-x}Co_{2x}$, $0 \le x \le 0.5$)," J. Mater. Chem., Vol. 17, pp. 2069-2077

[21] S. J. Shi, J. P. Tu, Y. Y. Tang, Y. X. Yu, Y. Q. Zhang, X. L. Wang, and C. D. Gu, "Combustion synthesis and electrochemical performance of $Li[Li_{0.2}Mn_{0.54}Ni_{0.13}Co_{0.13}]O_2$ with improved rate capability," J. Power Sources, Vol. 228, pp. 14-23

[22] A. Francis, K. Daniela, T. Michael, Z. Leila, G. Judith, L. Nicole, G. Gil, M. Boris, and A. Doron, "Synthesis of Integrated Cathode Materials $xLi_2MnO_3 \cdot (1-x)LiMn_{1/3}Ni_{1/3}Co_{1/3}O_2$ (x=0.3, 0.5, 0.7) and Studies of Their Electrochemical Behavior," J. Electrochem. Soc., Vol. 157, pp. A1121-A1126

[23] G. Y. Kim, S. B. Yi, Y. J. Park, and H. G. Kim, "Electrochemical behaviors of $Li[Li_{(1-x)/3}Mn_{(2-x)/3}Ni_{x/3}Co_{x/3}]O_2$ cathode series ($0<x<1$) synthesized by sucrose combustion process for high capacity lithium ion batteries," Mater. Res. Bull., Vol. 43, pp. 3543-3552

[24] S. J. Shi, J. P. Tu, Y. Y. Tang, Y. Q. Zhang, X. L. Wang, and C. D. Gu, "Preparation and characterization of macroporous $Li_{1.2}Mn_{0.54}Ni_{0.13}Co_{0.13}O_2$ cathode material for lithium-ion batteries via aerogel template," J. Power Sources, Vol. 240, pp. 140.

[25] F. Zhou, X. M. Zhao, A. Bommel, A. W. Rowe, and J. R. Dahn, "Coprecipitation Synthesis of $Ni_xMn_{1-x}(OH)_2$ Mixed Hydroxides," Chem. Mater., Vol. 22, pp. 1015-1021

[26] K. Lee, S. Myung, J. Moon, and Y. Sun, "Particle size effect of $Li[Ni_{0.5}Mn_{0.5}]O_2$ prepared by co-precipitation," Electrochim. Acta, Vol. 53, pp. 6033-6037

[27] H. Bang, B. Park, J. Prakash, Y. Sun, "Synthesis and electrochemical properties of $Li[Ni_{0.45}Co_{0.1}Mn_{0.46-x}Zr_x]O_2$ (x=0, 0.02) via co-precipitation method," J. Power Sources, Vol. 174, pp. 565-568

[28] L. Zhang, K. Jin, L. Wang, Y. Zhang, X. Li, and Y. Song, "High capacity $Li_{1.2}Mn_{0.54}Ni_{0.13}Co_{0.13}O_2$ cathode materials synthesized using mesocrystal precursors for lithium-ion batteries," J. Alloys Comp., Vol. 638, pp. 298-304

[29] Z. H. Lu, L. Y. Beaulieu, R. A. Donaberger, C. L. Thomas, J. R. Dahn, "Synthesis, Structure, and Electrochemical Behavior of $Li[Ni_xLi_{1/3-2x/3}Mn_{2/3-x/3}]O_2$," J. Electrochem. Soc., Vol. 149, pp. A778-A791

[30] M. M. Thackeray, S. H. Kang, C. S. Johnson, J. T. Vaughey, R. Benedek, and S. A. Hackney, "Li_2MnO_3-stabilized $LiMO_2$ (M=Mn, Ni, Co) electrodes for lithium-ion batteries," J. Mater. Chem., Vol. 17, pp. 3112-3125

[31] C. W. Park, S. H. Kim, I. Ruth Mangani, J. H. Lee, S. Boo, and J. Kim, "Synthesis and materials characterization of Li_2MnO_3-$LiCrO_2$ system nanocomposite electrode materials," Mater. Res. Bull., Vol. 42, pp. 1374-1383

[32] Z. Lu, and J. R. Dahn, "*In Situ* and *Ex Situ* XRD Investigation of $Li[Cr_xLi_{1/3-x/3}Mn_{2/3-2x/3}]O_2$ (x=1/3) Cathode material Batteries," J. Electrochem. Soc., Vol. 150, pp. A1044-A1051

[33] B. Hwang, R. Santhanam, and C. Chen, "Effect of synthesis conditions on electrochemical properties of $LiNi_{1-y}Co_yO_2$ cathode for lithium rechargeable batteries," J. Power Sources, Vol. 114, pp. 244-252

[34] R. Alcantara, P. Lavela, J. Tirado, R. Stoyanova, and E. Zhecheva, "Changes in Structure and Cathode Performance with Composition and Preparation Temperature of Lithium Cobalt Nickel Oxide," J. Electrochem. Soc., Vol. 145, pp. 730-736

[35] Z. Chang, Z. Chen, F. Wu, H. Tang, Z. Zhu, X. Z. Yuan, and H. Wang, "Synthesis and characterization of high-density non-spherical $Li(Ni_{1/3}Co_{1/3}Mn_{1/3})O_2$ cathode material for lithium ion batteries by two-step drying method," Electrochim. Acta, Vol. 53, pp. 5927-5933

[36] Z. L. Liu, A. S. Yu, and J. Y. Lee, "Synthesis and characterization of $LiNi_{1-x-y}Co_xMn_yO_2$ as the cathode materials of secondary lithium batteries," J. Power Sources, Vol. 81, pp. 416-419

[37] D. Mohanty, S. Kalnaus, R. A. Meisner, K. J. Rhodes, J. L. Li, E. A. Payzant, D. L. Wood, and C. Daniel, "Structural transformation of a lithium-rich $Li_{1.2}Co_{0.1}Mn_{0.55}Ni_{0.15}O_2$ cathode during high voltage cycling resolved by *in situ X*-ray diffraction," J. Power Sources, Vol. 229, pp. 239-248

[38] G. B. Liu, H. Liu, Y. F. Shi, "The synthesis and electrochemical properties of xLi_2MnO_3-(1-x)MO_2 ($M=Mn_{1/3}Ni_{1/3}Fe_{1/3}$) via co-precipitation method," Electrochim. Acta, Vol. 88, pp. 112-116

[39] B. H. Song, Z. W. Liu, M. O. Lai, and L. Lu, "Structural evolution and the capacity fade mechanism upon long-term cycling in Li-rich cathode material," Chem. Chem. Phys., Vol. 14, pp. 12875-12883

[40] W. S. Yoon, N. Kim, X. Q. Yang, J. McBreen, and C. P. Grey, "^{6}Li MAS NMR and in situ X-ray studies of lithium nickel manganese oxides," J. Power Sources, Vol. 119, pp. 649-653

[41] J. Zhang, X. Guo, S. Yao, W. Zhu, and X. Qiu, "Tailored synthesis of $Ni_{0.25}Mn_{0.75}CO_3$ spherical precursors for high capacity Li-rich cathode materials via a urea-based precipitation method," J. Power Sources, Vol. 238, pp. 245-250

[42] N. Yabuuchi, K. Yoshii, S. T. Myung, I. Nakai, and S. Komaba, "Detailed Studies of a High-Capacity Electrode Material for Rechargeable Batteries, Li_2MnO_3-$LiCo_{1/3}Ni_{1/3}Mn_{1/3}O_2$," J. Am. Chem. Soc., Vol. 133, pp. 4404-4419

[43] Z. Lu, and J. Dahn, "Understanding the Anomalous Capacity of $Li/Li[Ni_xLi_{(1/3-2x/3)}Mn_{(2/3-x/3)}O_2$ Cells Using *In Situ X*-Ray," Electrochem. Soc., Vol. 149, pp. A815-A822

[44] A. Robertson, and P. Bruce, "Overcapacity of $Li[Ni_xLi_{1/3-2x/3}Mn_{2/3-x/3}]O_2$ Electrodes," Electrochem. Solid State Lett., Vol. 7, pp. A294-A298

[45] A. R. Armstrong, M. Holzapfel, P. Novak, C. Johnson, S. Kang, M. Thackeray, and P. Bruce, "Demonstrating Oxygen Loss and Associated Structural Reorganization in the Lithium Battery Cathode $Li[Ni_{0.2}Li_{0.2}Mn_{0.6}]O_2$," J. Am. Chem. Soc., Vol. 128, pp. 8694-8698

[46] F. Wu, M. Wang, Y. Su, L. Bao, and S. Chen, "A novel method for synthesis of layered $LiNi_{1/3}Mn_{1/3}Co_{1/3}O_2$ as cathode material for lithium-ion battery," J. Power Sources, Vol. 195, pp. 2362-2367

[47] J. Zheng, S. Deng, Z. Shi, H. Xu, Y. Deng, Z. Zhang, and G. Chen, "The effects of persulfate treatment on the electrochemical properties of $Li[Li_{0.2}Mn_{0.54}Ni_{0.13}Co_{0.13}]O_2$ cathode material," J. Power Sources, Vol. 221, pp. 108-113

[48] J. J. Wang, G. Yuan, M. Zhang, B. Qiu, Y. Xia, and Z. Liu, "The structure, morphology, and electrochemical properties of $Li_{1+x}Ni_{1/6}Co_{1/6}Mn_{4/6}O_{2.25+x/2}$ ($0.1 \le x \le 0.7$) cathode materials," Electrochim. Acta, Vol. 66, pp. 61-66

[49] A. Ito, D. Li, Y. Sato, M. Arao, M. Watanabe, M. Hatano, H. Horie, and Y. Ohsaw, "Cyclic deterioration and its improvement for Li-rich layered cathode material $Li[Ni_{0.17}Li_{0.2}Co_{0.07}Mn_{0.56}]O_2$," J. Power Sources, Vol. 195, pp. 567-573

[50] J. Park, J. H. Seo, G. Plett, W. Lu, and A. M. Sastry, "Numerical Simulation of the Effect of the Dissolution of $LiMn_2O_4$ Particles on Li-Ion Battery Performance," Electrochem. Solid State Lett., Vol. 14, pp. A14-A18

[51] D. H. Jang, Y. J. Shin, and S. M. Oh, "Dissolution of Spinel Oxides and Capacity Losses in 4 V $Li/Li_xMn_2O_4$ Cells," J. Electrochem. Soc., Vol. 143, pp. 2204-2211

[52] M. Wohlfahrt-Mehrens, C. Vogler, and J. Garche, "Aging mechanisms of lithium cathode materials," J. Power Sources, Vol. 127, pp. 58-64

[53] M. D. Levi, K. Gamolsky, D. Aurbach, U. Heider, and R. Oesten, "On electrochemical impedance measurements of $Li_xCo_{0.2}Ni_{0.8}O_2$ and Li_xNiO_2 intercalation electrodes," Electrochim. Acta, Vol. 45, pp. 1781-1789

[54] S. A. Mamuru, K. I. Ozoemena, T. Fukuda, and N. Kobayashi, "Iron (II) tetrakis (diaquaplatinum) octacarbixyphthalocyanine supported on multi-walled carbon nanotube platform: an efficient functional material for enhancing electron transfer kinetics and electrocatalytic oxidation of formic acid," J. Mater. Chem., Vol. 20, pp. 10705-10715

[55] H. W. Ha, N. J. Yun, and K. Kim, "Improvement of electrochemical stability of $LiMn_2O_4$ by CeO_2 coating for lithium-ion batteries," Electrochim. Acta, Vol. 52, pp. 3236-3241

[56] Q. Cao, H. P. Zhang, G. J. Wang, Q. Xia, Y. P. Wu, and H. Q. Wu, "A novel carbon-coated $LiCoO_2$ as cathode material for lithium ion battery," Electrochem. Commun., Vol. 9, pp. 1228-1232

[57] C. J. Jafta, K. I. Ozoemena, M. K. Mathe, and W. D. Roos, "Synthesis, characterisation and electrochemical intercalation kinetics of nanostructured aluminium-doped $Li[Li_{0.2}Mn_{0.54}Ni_{0.13}Co_{0.13}]O_2$ cathode material for lithium ion battery," Electrochim. Acta, Vol. 85, pp. 411-422

[58] K. G. Gallagher, J. R. Croy, M. Balasubramanian, M. Bettge, D. P. Abraham, A. K. Burrell, and M. M. Thackeray, "Correlating hysteresis and voltage fade in lithium- and manganese-rich layered transition-metal oxide electrodes," Electrochem. Commun., Vol. 33, pp. 96-98